Pathology - Research and Practice 215 (2019) 963–976

Contents lists available at ScienceDirect

Pathology - Research and Practice

journal homepage: www.elsevier.com/locate/prp

Expression level and prospective mechanism of miRNA-99a-3p in head and neck squamous cell carcinoma based on miRNA-chip and miRNA-sequencing data in 1, 167 cases

Gan-Guan Wei[a,1], Wan-Ping Guo[b,1], Zheng-Yi Tang[a], Sheng-Hua Li[c], Hua-Yu Wu[b,**], Long-Cheng Zhang[a,*]

[a] Department of Otolaryngology Head and Neck Surgery, 303 Hospital of PLA Guangxi Zhuang Autonomous Region, Nanning, China
[b] Department of Cell Biology and Genetics, School of Pre-clinical Medicine, Guangxi Medical University, Nanning, Guangxi Zhuang Autonomous Region, China
[c] Department of Urology, The First Affiliated Hospital of Guangxi Medical University, Nanning, Guangxi Zhuang Autonomous Region, China

ARTICLE INFO

Keywords:
MiR-99a-3p
Head and neck squamous cell carcinoma
MiRNA-chip
MiRNA-sequencing
Pathway

ABSTRACT

Background: The role of miR-99a-3p in Head and neck squamous cell carcinoma (HNSCC) has not been reported. Therefore, in this study, we examined the expression level and its molecular mechanisms of miR-99a-3p in HNSCC.

Materials and methods: MiR-99a-3p-related miRNA-chip and miRNA-sequencing data were collected. We then carried out meta-analyses to pool the standard mean difference (SMD) value and generate a summarized receiver operating characteristic (sROC) curve. MiR-99a-3p mimic was transfected into FaDu cells and those genes influenced by miR-99a-3p were gathered. The target genes were also predicted from 12 tools through miRwalk2.0, and combined with differentially expressed genes in HNSCC from the The Cancer Genome Atlas and Genotype-Tissue Expression sequencing databases. FunRich and DAVID were used for the pathway signaling analyses for the potential targets of miR-99a-3p in HNSCC.

Results: The SMD was -0.30 (95% CI: -0.51, -0.08) in the fixed-effect model and -0.28 (95% CI: -0.67, 0.10) in the random-effect model (I2 = 60%), indicating a reduced expression level of miR-99a-3p in HNSCC tissues based on 1167 cases. In the sROC curve, the area under the curve (AUC) was 0.77 (95% CI: 0.73, 0.81). The 251 potential targets of miR-99a-3p were enriched in several pathways related to cancer, with the “Pathways in cancer” standing at the top. vascular endothelial growth factor A was selected as an example with up-regulated trend in HNSCC tissues.

Conclusion: MiR-99a-3p exhibits a significant lower expression status in HNSCC, and this reduced or deletion status promotes the malignant progression of HNSCC. However, its molecular mechanism is still unclear and requires further investigation.

1. Introduction

Head and neck squamous cell carcinoma (HNSCC) is the sixth most prevalent cancer globally. There are approximately 550,000 newly diagnosed patients and 300,000 fatalities each year. Although research in the HNSCC field has progressed significantly over the last several years and treatment approaches have improved, HNSCC still has a 50% elapse rate [1–6].

The pathogenic factors of HNSCC are the use of tobacco and alcohol, which are associated with 75% of HNSCC cases. HNSCC is also associated with human papillomavirus (HPV) infection, and HPV infection is clearly related to a subset of HNSCC cases [7,8]. The occurrence and development of HNSCC is closely related to many molecular mechanisms, but further research is needed, particularly regarding the relationship between microRNAs (miRNAs) and HNSCC [9].

MiRNAs are small, single-stranded, non-coding RNAs (18–23

* Corresponding author at: Department of Otolaryngology Head and Neck Surgery, 303 Hospital of PLA, 52 Zhiwu Road, Guangxi Zhuang Autonomous Region, Nanning, China.
** Corresponding author at: Department of Cell Biology and Genetics, School of Pre-clinical Medicine, Guangxi Medical University, 22 Shuangyong Road, Guangxi Zhuang Autonomous Region, Nanning, China.
E-mail addresses: wuhuayu0418@hotmail.com (H.-Y. Wu), zhanglch9923@163.com (L.-C. Zhang).
[1] Contributed equally as first authors.

https://doi.org/10.1016/j.prp.2019.02.002
Received 27 November 2018; Received in revised form 20 January 2019; Accepted 1 February 2019
0344-0338/

Table 1
Basic statistics of GEO miRNA-chips.

Accession	HNSCC		controls		p	t	TP	FP	FN	TN
	n	Mean ± SD	n	Mean ± SD						
GSE28100	17	0.215 ± 1.002	3	−0.098 ± 0.068	0.604	0.529	6	0	11	3
GSE32906	16	205.414 ± 120.524	6	158.403 ± 30.516	0.363	0.931	7	1	9	5
GSE32960	312	8.713 ± 0.284	18	8.637 ± 0.325	0.271	1.103	270	14	42	4
GSE34496	44	1.477 ± 0.5	25	1.6 ± 0.482	0.324	0.994	11	1	33	24
GSE36682	62	8.625 ± 0.299	6	9.094 ± 0.428	< 0.001	3.531	53	1	9	5
GSE41268	7	−3.229 ± 0.076	3	−3.029 ± 0.334	0.145	1.615	3	0	4	3
GSE43329	31	68.694 ± 7.547	19	69.736 ± 0.416	0.552	0.599	2	0	29	19
GSE45238	40	114.222 ± 60.942	40	201.892 ± 122.947	< 0.001	4.041	33	14	7	26
GSE46172	4	−2.809 ± 0.532	4	−3.1 ± 0.37	0.404	0.898	4	4	0	0
GSE62819	5	1.943 ± 0.531	5	2.046 ± 0.646	0.788	0.278	5	4	0	1
GSE69002	3	3.118 ± 0.129	4	3.179 ± 0.088	0.486	0.751	2	1	1	3

nucleotides) that inhibit translation or cleavage of RNA transcripts in a sequence-related behavior. MiRNAs can execute as controlling fine-tuners of protein-encoding or after transcription of non-coding RNAs [10]. Growing evidence suggests aberrantly expressed miRNAs are closely related to human disease pathogenesis, including HNSCCs. However, many miRNAs that may play a role in HNSCC have yet to be discovered [9,11–14].

Among all the miRNAs, miRNA-99a-3p (miR-99a-3p) has rarely been studied in tumors. At present, one report found that over-expression of miR-99a-3p is associated with improved progression-free survival (PFS) and/or overall survival (OS) in metastatic colorectal cancer (mCRC), and overexpression of miR-99a-3p can also be used as a predictive biomarker for chemotherapy response in mCRC [15]. Studies have documented miR-99a-3p is decreased in endometrioid endometrial carcinoma [16] and prostate cancer [17]. Moreover, transfection of miR-99a-3p in vitro largely suppresses cell growth, mobility, and infiltration in prostate cancer cells [18]. The expression level and role of miR-99a-3p in HNSCC, as well as its molecular mechanisms, have not been reported. Therefore, in this study, we recalculated the miRNA-chip and miRNA-sequencing data to examine the clinical value of miR-99a-3p in HNSCC. As a single miRNA can regulate hundreds of thousands of mRNAs, we also intervened in the probable target genes and pathways of miR-99a-3p. The gene chip data after artificially elevating miR-99a-3p were mined to obtain the affected differentially expressed gene (DEG) group, and later intersected with those DEGs found to play a role in HNSCC through RNA-sequencing. This comprehensive understanding of the prospective target gene profile of miR-99a-3p provides a foundation for further research on the regulation mechanism of miR-99a-3p in HNSCC.

2. Materials and methods

2.1. Clinical significance of miR-99a-3p in HNSCC

2.1.1. miR-99a-3p-related miRNA-chip and miRNA-sequencing data collection

Based on the Gene Expression Omnibus (GEO), ArrayExpress, and Sequence Read Archive (SRA), we searched for miRNA-chip and miRNA-sequencing data using ((SCC OR HNSCC OR “squamous cell carcinoma” OR “squamous cell cancer”)) AND (oropharyngeal OR oropharynx OR “head and neck” OR “oral cavity” OR nasopharynx OR hypopharynx OR laryngopharynx OR oral OR larynx OR laryngopharyngeal OR laryngeal OR pharyngeal OR laryngeal OR tongue OR tonsil OR tonsillar OR nose OR “nasal sinus” OR lip OR cheek OR “nasal cavity” OR “paranasal sinuses” OR palatal OR buccal)) AND (microRNA OR microRNA OR miRNA OR miRNA OR MIR OR miR)) with “entry type” and “organisms” restricted to “series” and “Homo sapiens,” respectively. The miRNA-chip and miRNA-sequencing data that met the following criteria were included: (1) human data sources; (2) expression of miR-99a-3p in HNSCC and normal groups from upper aerodigestive tract mucosa tissues. No less than three samples in each group were selected. The expression level of miR-99a-3p was extracted and presented as mean value and standard deviation (SD). We assessed the difference in miR-99a-3p between cancerous and non-cancerous groups using the student’s t-test, and ROC was performed using SPSS 23.0.

2.1.2. miRNA-sequencing data mining

The Cancer Genome Atlas (TCGA) database provided the clinical characteristics and expression data of miR-99a-3p for archived HNSCC patients and normal upper aerodigestive tract mucosa controls, which were downloaded via online tools provided by UCSC [19–21]. Expression data from IlluminaHiseq and IlluminaGA were both previously normalized to a log2(RPM + 1) scale and input into GraphPad Prism5.0. Additionally, we determined the prognostic value of miR-99a-3p for HNSCC by performing an OS analysis based on the clinical phenotype file. Other statistical methods are mentioned above.

2.1.3. Retrieval of the literature

We searched NCBI PubMed, Wiley Online Library, Web of Science, Science Direct, Cochrane Central Register of Controlled Trials, Google Scholar, EMBASE, Ovid, LILACS, Chinese CNKI, Chong Qing VIP, Wan Fang, and China Biology Medicine Disc for additional data using the aforementioned strategy. Original studies providing miR-99a-3p expression data that could be summarized as mean value and standard deviation as well as sample numbers of both HNSCC and non-cancerous groups were included.

2.1.4. Meta-analyses of the clinical implication of miR-99a-3p in HNSCC

To obtain a comprehensive overview of the expression level of miR-99a-3p in HNSCC, we carried out meta-analyses with all data collected from multiple sources. We utilized R Project (Version 3.4) to conduct a continuous variable meta-analysis with a fixed-effect model and a

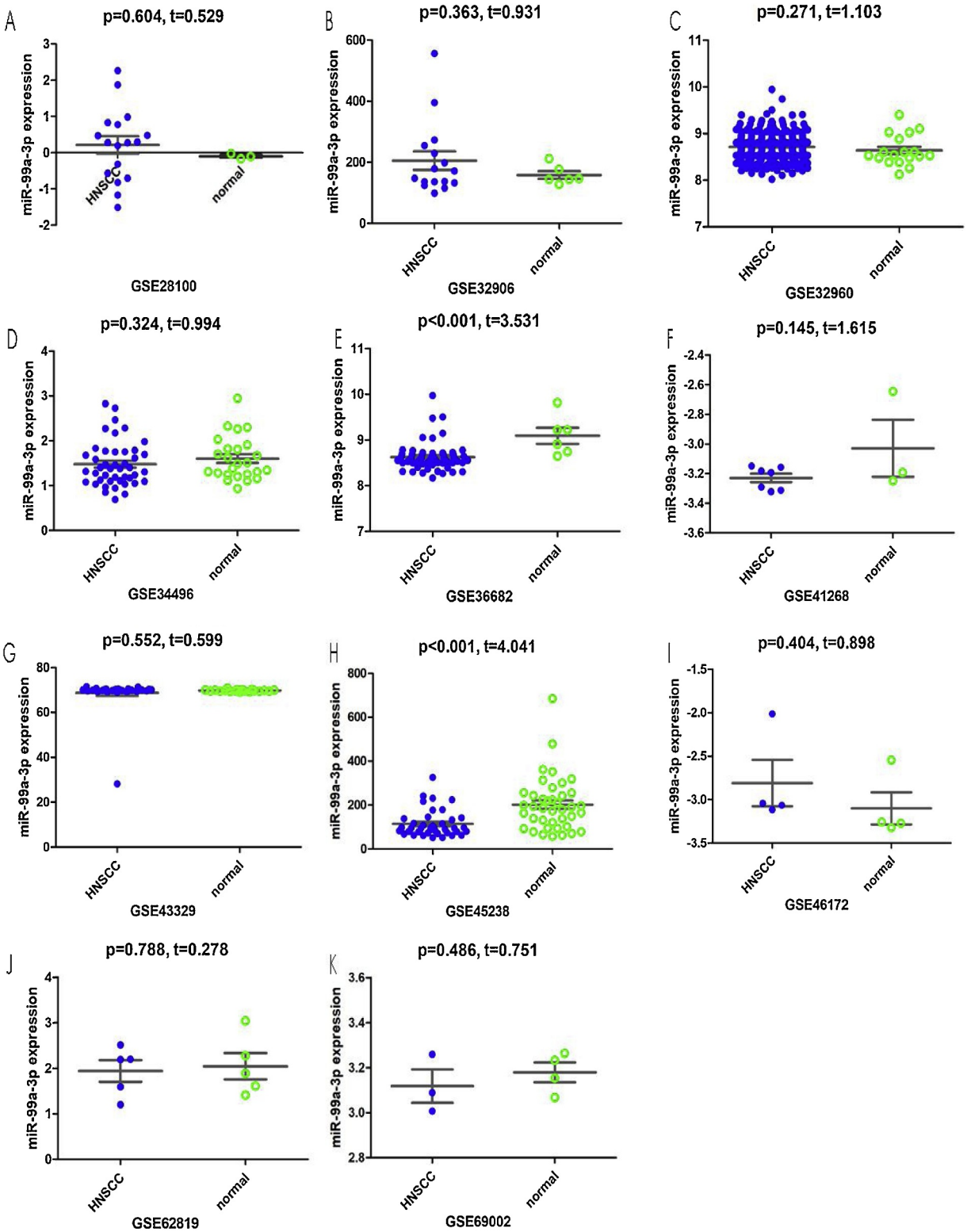

Fig. 1. Scatter diagrams of GEO miRNA-chips with miR-99a-3p expression in HNSCC (A. GSE28100, B. GSE32906, C. GSE32960, D. GSE34496, E. GSE36682, F. GSE41268, G. GSE43329, H. GSE45238, I. GSE46172, J. GSE62819, K. GSE69002).

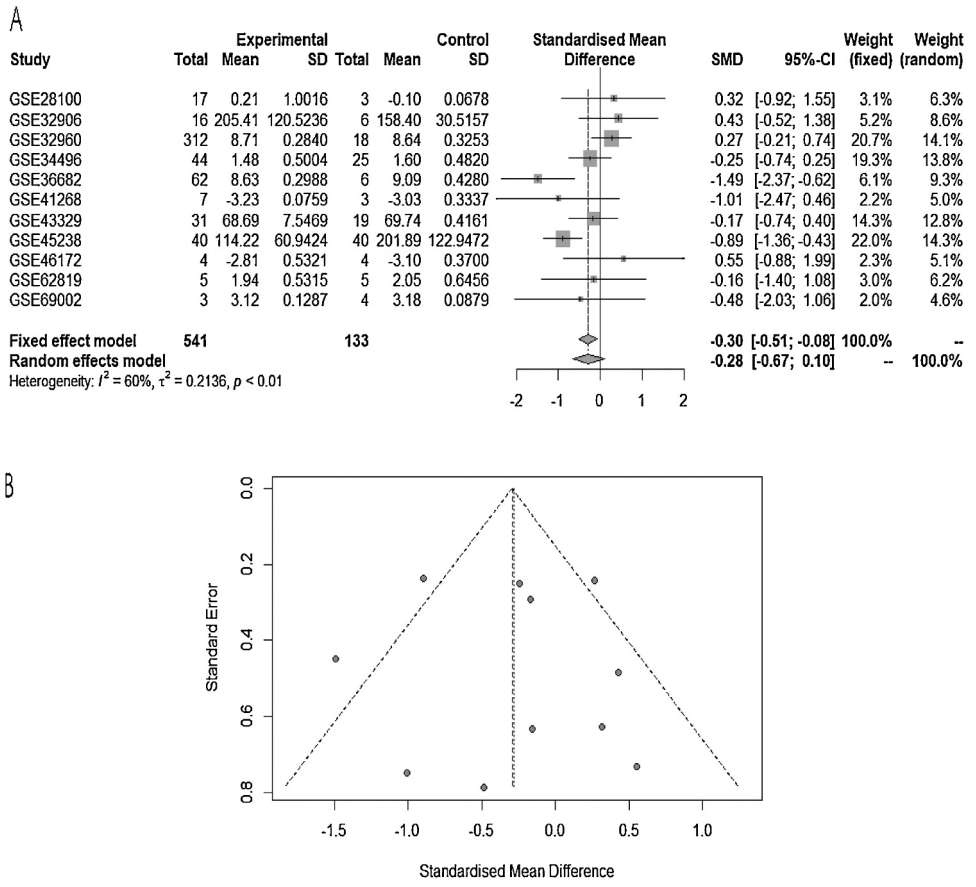

Fig. 2. Meta-analysis based on miRNA-chip data (A is the combined SMD and 95% CI calculated with fix-effect model and random-effect model; B is the funnel plot).

random-effect model to pool the standard mean difference (SMD) value and 95% confidence interval (95% CI). We carried out a sensitivity analysis when the heterogeneity was non-ignorable ($I^2 > 50\%$). In addition, we constructed a funnel plot to test publication bias. Furthermore, we applied STATA 12.0 to generate a summarized receiver operating characteristic (sROC) curve [22].

2.2. Potential pathways of miR-99a-3p in HNSCC

2.2.1. Prediction of target genes of miR-99a-3p in HNSCC

To further assess the potential biological character of miR-99a-3p in HNSCC, we first collected DEGs via the microarrays from GSM2279806, which was transfected with miR-99a-3p mimic into FaDu cells and those predicted target genes from 12 prediction tools through miRwalk2.0 [23]. Additionally, we acquired DEGs in HNSCC from the TCGA and Genotype-Tissue Expression (GTEx) sequencing databases as provided by Gene Expression Profiling Interactive Analysis (GEPIA) [24–26]. Genes from GSM2279806 and GEPIA were extracted with the expression value of $\log_2FC < 0$ and $\log_2FC > 1$ respectively, while genes crossing at least two prediction tools in miRwalk2.0 were also included. Finally, the putative target genes collected from the reported literature and the overlapping genes derived from GSM2279806, TCGA/GTEx, and the miRwalk2.0 prediction were regarded to be the likely target genes of miR-99a-3p in HNSCC.

2.2.2. Potential mechanism of miR-99a-3p in HNSCC

Based on the predicted target genes, we further explored the underlying function of miR-99a-3p in HNSCC. We used FunRich, a functional enrichment analysis software, to perform GO annotation analysis [27–30]. Kyoto Encyclopedia of Genes and Genomes (KEGG) pathways were also analyzed via DAVID [31–35]. A PPI network was constructed using STRING to reveal the potential protein interactions among the target genes, which permitted us to filtrate the possible hub genes of miR-99a-3p in HNSCC [36–39]. The mRNA and protein levels of several hub target genes were revealed as likely targets of miR-99a-3p in HNSCC using data from TCGA, GTEx, and The Human Protein Atlas (THPA) [24,40–44]. In THPA, squamous epithelial cells from normal oral mucosa and respiratory epithelial cells from nasopharynx mucosa were used as upper aerodigestive tract mucosa controls for HNSCC. The procedure of tissue microarray and immunohistochemistry were performed in a standard protocol according to the study criteria [40–42].

3. Results

3.1. Data extracted from GEO, ArrayExpress, TCGA, and publications

Of the 21 miRNA-chips datasets included after the preliminary searching, 11 miRNA-chips (GSE28100, GSE32906, GSE32960, GSE34496, GSE36682, GSE41268, GSE43329, GSE45238, GSE46172,

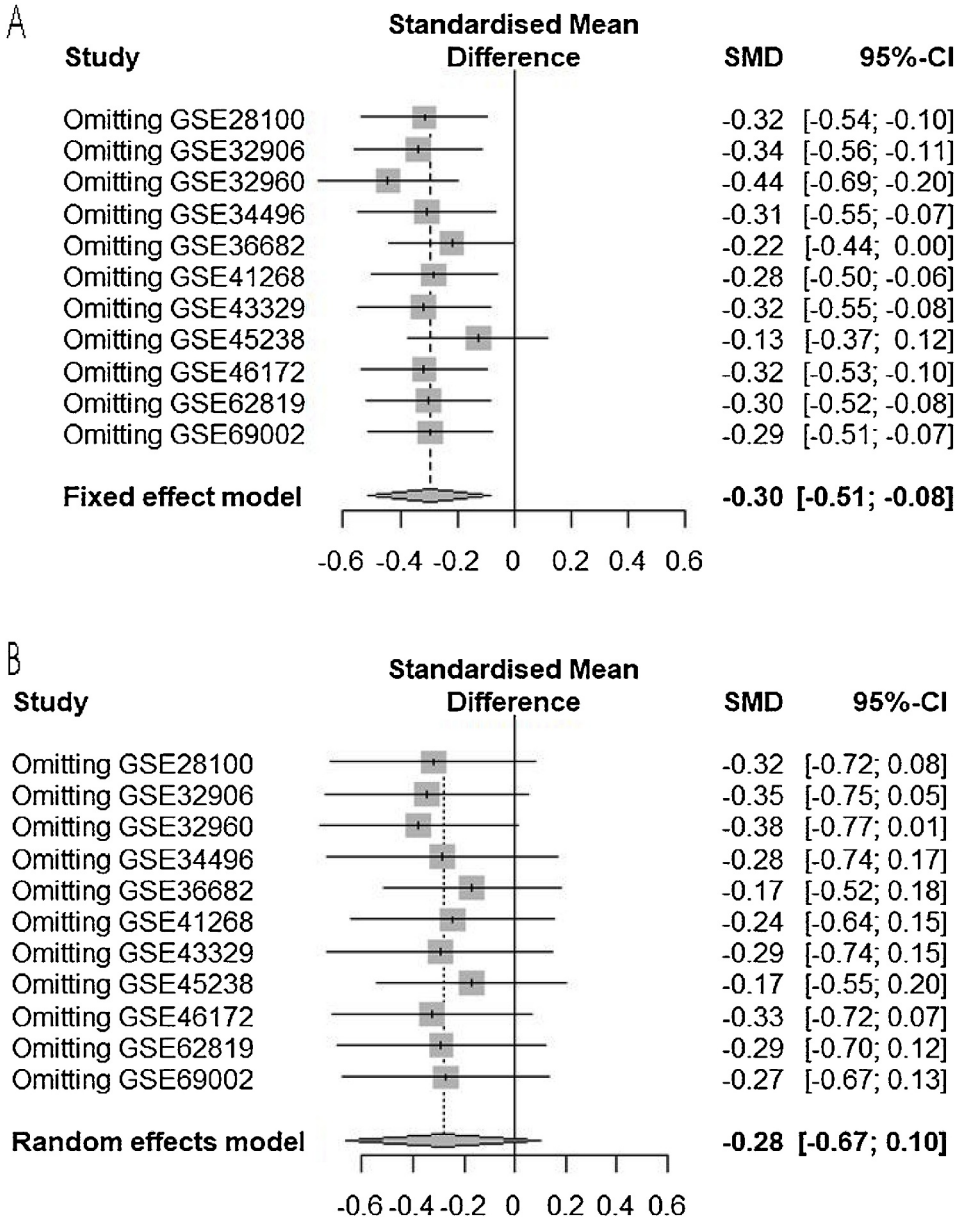

Fig. 3. Sensitivity analysis of the meta-analysis based on miRNA-chip data (A is the fix-effect model; B is the random-effect model).

GSE62819, and GSE69002) met the final criteria, with 674 HNSCC cases and 133 non-cancerous upper aerodigestive tract mucosa samples involved. TCGA provided the expression data for mature miR-99a-3p of 493 HNSCC (461 from the IlluminaHiseq dataset and 32 from the IlluminaGA dataset) and 44 control samples, as well as the clinicopathological features of HNSCC patients. No publications met our requirements. Thus, we conducted the comparison of miR-99a-3p expression levels in HNSCC and control groups, and analyzed its clinical value, based on these 1167 HNSCC cases.

3.2. Expression level of miR-99a-3p assessed by a meta-analysis calculating SMD

The mean, standard deviation, and cases numbers of miR-99a-3p expression in cancerous and non-cancerous upper aerodigestive tract mucosa tissues were calculated for each chosen chip (Table 1, Fig. 2); the expression levels are shown in the scatter diagrams depicted in Fig. 1. According to the continuous variable meta-analysis, the SMD was -0.30 (95% CI: -0.51, -0.08) in the fixed-effect model and -0.28 (95% CI: -0.67, 0.10) in the random-effect model (I^2 = 60%), indicating a reduced expression level of miR-99a-3p in HNSCC tissues. No

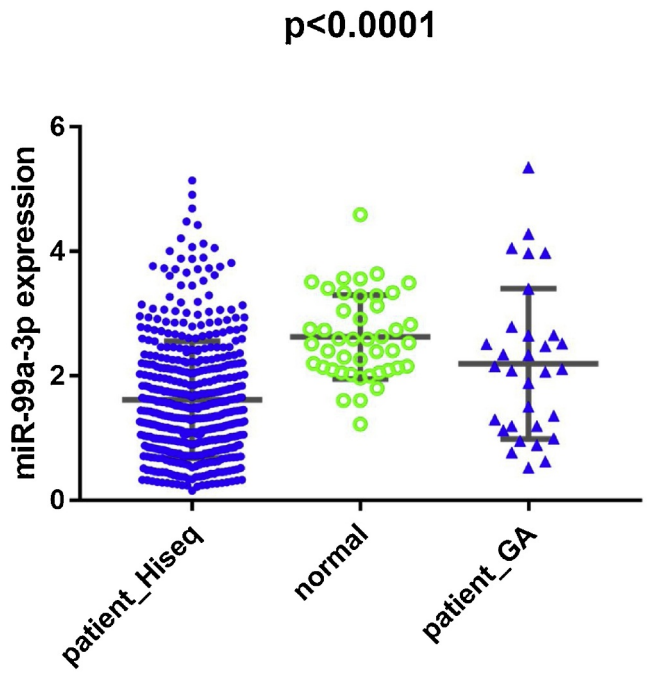

Fig. 4. Scatter diagram of TCGA miRNA-sequencing data with miR-99a-3p expression in HNSCC.
Both IlluminaHiseq and IlluminaGA are included.

publication bias was found after constructing the funnel plot ($p = 0.873$; Fig. 3). The results also showed expression of miR-99a-3p in HNSCC groups was lower than control groups for the TCGA datasets ($p < 0.0001$; Fig. 4).

3.3. Expression level of miR-99a-3p assessed by a meta-analysis calculating sROC

We further tested the clinical implications of miR-99a-3p by calculating the AUC of the sROC. Based on miRNA-chips and miRNA-sequencing data, the true positive (TP), false positive (FP), false negative (FN), and true negative (TN) were calculated (Table 1). According to our results, the combined sensitivity, specificity, positive likelihood ratio, negative likelihood ratio, and odds ratio were 0.65 (95% CI: 0.39, 0.85), 0.79 (95% CI: 0.42, 0.95), 3.11 (95% CI: 1.16, 8.36), 0.44 (95% CI: 0.28, 0.70), and 7.06 (95% CI: 2.84, 17.58). In the sROC curve, the area under the curve (AUC) was 0.77 (95% CI: 0.73, 0.81; Fig. 5). For the TCGA dataset, we also plotted the ROC curves, and the AUC was 0.817 (95% CI: 0.77, 0.86) and 0.807 (95% CI: 0.76, 0.85; Fig. 6) when the HNSCC patients recorded in the IlluminaGA dataset were included.

Our analysis indicates miR-99a-3p might play a vital protective role in the tumorigenesis of HNSCC which on the other side exhibited a lack of reliability due to inadequate body fluid samples. Furthermore, the hazard ratio (HR) was 1.62 ($p = 0.002$, 95% CI: 1.19, 2.21) and 1.77 ($p < 0.001$, 95% CI: 1.31, 2.41) for lower expression of miR-99a-3p by OS analysis, which verifies a lower expression level of miR-99a-3p could indicate a lower survival rate.

3.4. Potential biological role of miR-99a-3p in HNSCC

Fig. 7 and Table 2 show the 247 intersecting genes and 4 relevant reported genes considered to be promising target genes of miR-99a-3p. GO annotation items were separated into three parts: biological processes, cellular components, and molecular functions; the 10 most significantly related items for each part are shown in Fig. 6. A KEGG pathway analysis demonstrates 251 promising target genes were significantly enriched in 8 biological pathways ($p < 0.01$), of which pathways in cancer was the most significant biological pathway (Fig. 8, Table 3). Moreover, calculated and filtered by Cytoscape, the PPI network reveals VEGFA, PIK3CD, IGF1R, MTOR, CDKN2A, GNA12, MET, GNB5, RAC2, STAT1, TNFSF10, HIF1A, MMP14, CDKN3, FCGR3A, and MAPK12 were considered to be hub genes of miR-99a-3p in HNSCC (Fig. 9; all degrees of edges ≥ 10). The top hub gene vascular endothelial growth factor A (VEGFA), with 27 connections with other genes, was selected to show the mRNA and protein levels in HNSCC, both of which reveal an up-regulated trend (Fig. 9). However, due the limited sample size from Protein Atlas, no statistical analysis was possible. The increased level of VEGFA (Fig. 10) should be validated by more samples.

4. Discussion

The expression abundance and clinical significance of miR-99a-3p in HNSCC have not been reported previously, and its molecular mechanism is also unknown. For the first time, this study used miRNA-chip and miRNA-sequencing data to show miR-99a-3p presented a significant low expression trend in 1167 cases of HNSCC as compared to that in upper aerodigestive tract mucosa controls. Furthermore, lower expression of miR-99a-3p could also predict poorer prognosis, suggesting a decrease or deletion may play a paramount role in the occurrence and progression of HNSCC. These clinical effects of miR-99a-3p may be achieved by different target genes and signaling pathways. The bioinformatics methods used in this study provide a new direction for the study of miRNAs in HNSCC.

The role of miR-99a-3p in diseases is not a frequent topic in the literature. To date, the expression and function of miR-99a-3p in cancers has been reported only in a small number of tumor types. These studies all pointed to the protective role of miR-99a-3p in the development and progression of malignancies. The expression level of miR-99a-3p has been revealed in only two cancer types, endometrioid endometrial and prostate cancer [16,17]. MiR-99a-3p expression level was observed to be down-regulated in endometrioid endometrial carcinoma tissues as compared to non-cancerous controls, which was confirmed by both RNA sequencing and real-time quantitative PCR [16]. We previously found markedly reduced miR-99a-3p levels in cancerous versus non-cancerous prostate tissues based on miRNA-chip and miRNA-sequencing data [17]. In the current study, the constant reduced expression level of miR-99a-3p was also detected in HNSCC tissues, indicating miR-99a-3p levels could be reduced during HNSCC carcinogenesis, similar to endometrioid endometrial and prostate cancer. Multiple experimental methods were used in the current study, including miRNA-chips, miRNA-sequencing, and meta-analyses involving SMD and sROC, which increases the credibility of the results. Moreover, the finding of a lower expression level of miR-99a-3p in HNSCC was based on a large sample size involving 1167 cases from different districts. However, real-time RT-qPCR, the most common

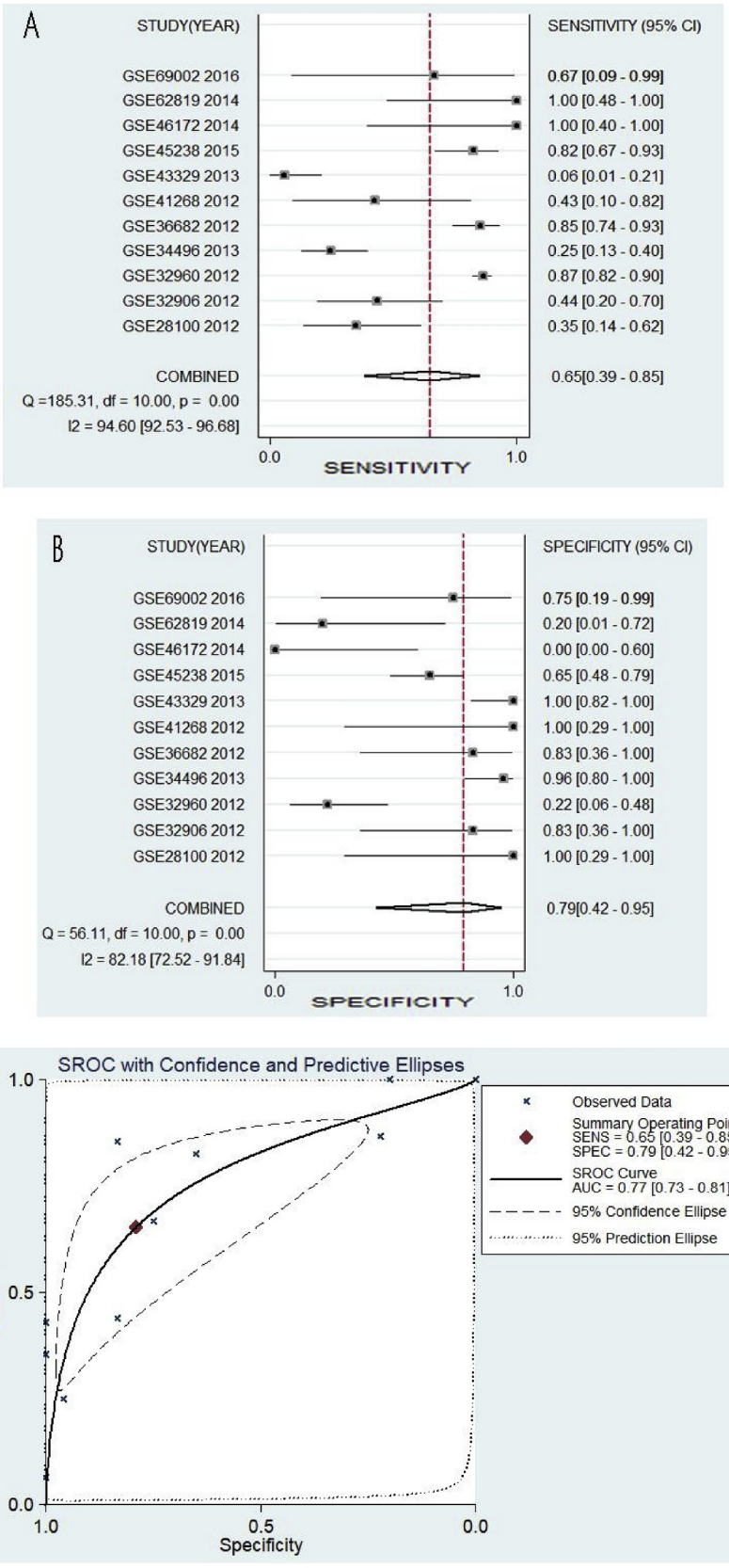

Fig. 5. Distinguishing value of miR-99a-3p for HNSCC based on miRNA-chip data (A is the sensitivity analysis; B is the specificity analysis; C is the sROC curve).

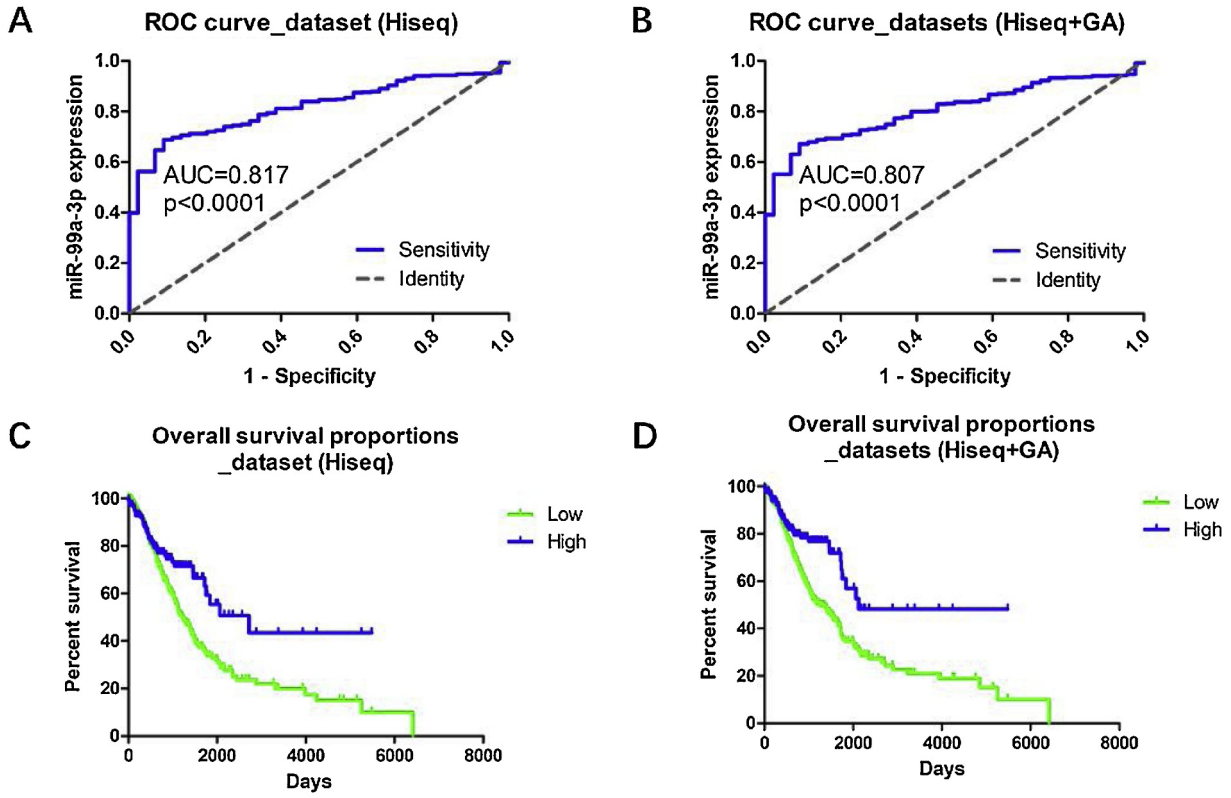

Fig. 6. Clinical value of miR-99a-3p in HNSCC based on TCGA miRNA-sequencing data (A and B are ROC curves; C and D are overall survival analyses).

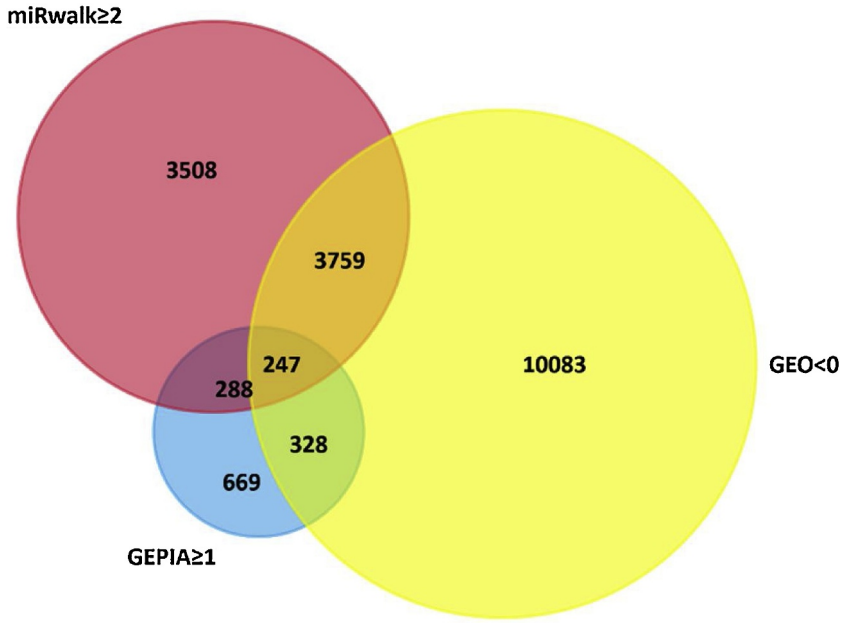

Fig. 7. Venn diagram of the potential target genes of miR-99a-3p in HNSCC.

Table 2
Promising target gene list of miR-99a-3p in HNSCC.

	Genes							
Validated genes in other diseases	MTMR3	IGF1R	MTOR	HOXA1				
Predicted targets by analytical integration	TGFBI	ARSI	CTSL	XPR1	SLC1A4	TRIO	RECQL	PRELID2
	COL5A1	C12orf75	MET	LOX	ISLR	MTHFD2	YDJC	JOSD1
	SPARC	NRG1	HTR7	F2RL2	WIPF1	PRNP	ECE1	SCARF2
	IGF2BP2	BCAS4	AGTRAP	CNGB1	STAT2	GOLGA8A	KIAA0930	LPAR2
	FKBP10	COL5A3	NDE1	TRPV3	ETS1	GUCY1B3	HSF4	WFDC5
	HMGA2	BASP1	MICAL2	SLC7A5	TNFRSF25	PPP4R4	MAN1B1	SLFN11
	HTRA3	DCBLD1	STARD4	LILRB4	GALNT2	CHIT1	GOLIM4	NUAK1
	NXPH4	TPBG	KIRREL	RAB34	SOAT1	PIK3CD	CBX2	SLC44A1
	CERCAM	MSC	THEMIS2	KIF26B	ABL2	CDR2L	PLEKHG2	NFKBIE
	PMEPA1	MMP14	DCBLD2	MAPK12	UCHL1	MFSD10	LAYN	ENY2
	COL11A1	GNA12	GPR153	RGS20	B3GNT9	GFPT2	TTC7B	RELB
	ADAM12	CTSC	C11orf84	C10orf35	ARSJ	MCTP1	RNF213	CERS2
	CDKN2A	SCD5	KLHL5	DNMT3B	LIMA1	ALOXE3	SLC6A8	HIP1
	LCE3D	LAMP3	YEATS2	MTHFD1L	NFE2L3	SLC28A3	DENND1A	ORAI2
	HOXA10	THSD1	SLC39A14	PDE7A	SEMA4F	TBX18	DENND5A	POFUT1
	ITGA6	LBH	FZD6	LHFPL2	HEXA	H2AFV	TGIF1	SAMD9L
	TNC	WDR72	DERL3	LRRC8C	ARHGEF39	FGF11	DOK3	SGPP1
	SH2D5	FCGR3A	NDRG1	SHOX2	VEGFA	RGS3	APH1B	DPH7
	IGF2BP3	KYNU	PLEKHG4B	FAM83A	TP63	GNB5	PVR	NRP1
	TMEM132A	IGFBP3	MYO5A	MFAP5	CASK	NRBP2	MSR1	FKBP14
	STC2	CDKN3	FMNL3	PABPC1L	TMEM2	ARFGAP1	LPAR3	CHST7
	PHLDB2	CLIC4	HOXD8	ATP6V1C1	HIF1A	SKA2	AP2M1	IL18BP
	CDH3	SCRN1	LRP12	NEK2	CBX3	SH3PXD2B	TNFSF10	PDK1
	HOMER3	KLF7	FBLIM1	STON2	HAP1	PRTFDC1	CYGB	ENTPD7
	PTK7	TRAM2	PYGL	CSGALNACT2	MME	ADAM23	GOLT1B	NAGS
	RAC2	COL17A1	MSN	SMS	POLE	C5AR1	CEP170	OLR1
	IL36G	SLC38A5	SLAMF8	ATP13A3	SIAH1	BLOC1S3	OSBPL3	RNASE7
	CAV1	FLRT2	OLFML2A	CCDC71L	APBB2	BMP2	PAPLN	ABCG1
	MFI2	SPRY4	CBLB	TNFAIP3	JAG1	SKIL	MB21D2	SLC12A8
	STAT1	ARPC1B	RAB31	ELF4	ANTXR2	TNFAIP8L1	AGO2	ULK1
	BMP1	RGS4	PRSS23	DDX58	E2F7	GLS	PTPRH	

method used to detect miRNA, should be used in the future to verify these findings.

Although there are only a few studies on miR-99a-3p, they incorporate the prediction of tumor progression and therapeutic effects. They reveal the higher the expression of miR-99a-3p, the better the prognosis of mCRC patients. The higher expression of miR-99a-3p in mCRC also led to better responses to standard fluoropyrimidine-based chemotherapy. Therefore, miR-99a-3p may be a protective factor in the development of colon and rectal cancer [15]. This study reveals similar findings. In HNSCC, when the expression of miR-99a-3p increased, patients' prognosis improved. The decreased expression of miR-99a-3p was also a predictor of HNSCC survival. However, the prognostic value of miR-99a-3p was derived from a single cohort, which could be confirmed by meta-analysis. This protective role of miR-99a-3p will need to be corroborated by further studies.

Because miRNAs cannot encode proteins, they need to modulate different target genes to function. As miR-99a-3p has not been reported in HNSCC, its target genes are unknown. This study relied on a number of approaches to predict the potential target genes of miR-99a-3p in HNSCC. The first was to overexpress miR-99a-3p by transfection in FaDu, a hypopharyngeal squamous cell carcinoma cell line, and obtained the genes directly affected by miR-99a-3p using a gene chip. The second part of the gene group was compiled using target prediction software. The third included genes abnormally expressed in HNSCC tissues, because they potentially affect the development of HNSCC. We also included genes confirmed to be miR-99a-3p targets in other diseases. The 251 genes obtained are most likely to be the real target genes of miR-99a-3p in HNSCC. We chose to display mRNA and protein levels from the top hub gene VEGFA in the PPI network, as they were most likely to be highly expressed. Moreover, VEGFA has been shown to play a role in promoting cancer in HNSCC [45–47]. More tests are required to verify the relationships between miR-99a-3p and the targets, such as validation with clinical samples, in vitro dual luciferase report assays, and in vivo experiments.

Although this study was the first to summarize the under-expressed status of miR-99a-3p in HNSCC, further work is required. First, non-invasive detection is preferred for clinical diagnosis of tumors; this will be needed if miRNA is to be used as a diagnostic tool. Currently, the miR-99a-3p level has not been detected in patients' bodily fluids, although this should be tested in the future. Second, the potential target genes were predicted by computational biology tools, and must be substantiated. Third, the relationships between miR-99a-3p and its prospective targets also require clinical verification in patients. Fourth, one of the mechanisms of miRNA is to influence the protein level of target genes, which was lacking in the current study. Thus, the prospective targets in the current study do not represent all possibilities.

In conclusion, this study used miRNA-chip and miRNA-sequencing technology to determine miR-99a-3p exhibits a significant lower expression status in HNSCC, and this reduced or deletion status promotes the malignant progression of HNSCC. However, its molecular mechanism is still unclear and requires further investigation.

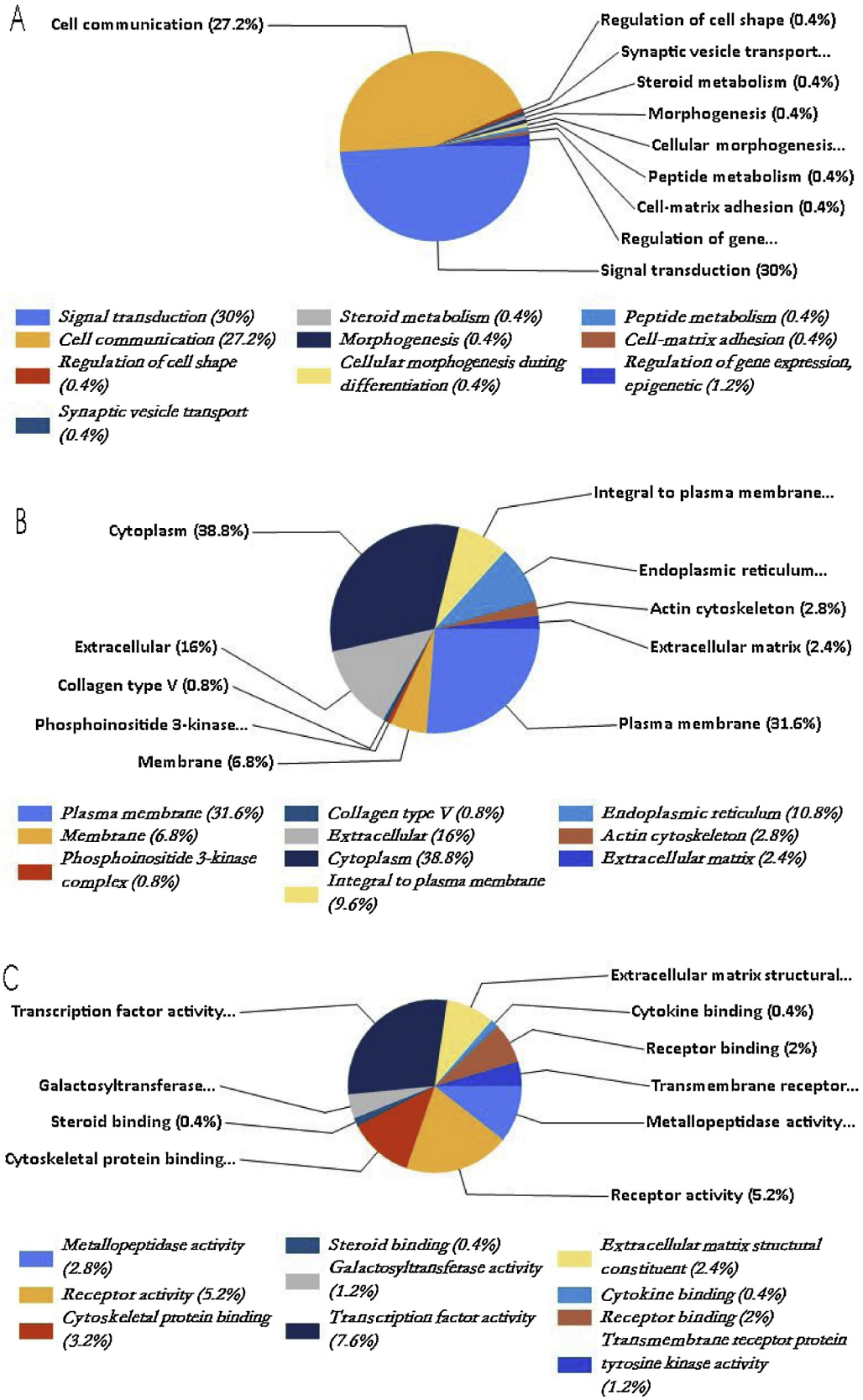

Fig. 8. GO annotation analysis of miR-99a-3p target genes in HNSCC (A is biological processes; B is cellular components; C is molecular functions).

Table 3
The most significant KEGG pathways of miR-99a-3p in HNSCC ($p < 0.01$).

KEGG terms	Count	%	P-value	Genes
Pathways in cancer	18	0.0452	7.36E-05	BMP2, MET, GNA12, PIK3CD, FGF11, LPAR3, LPAR2, STAT1, FZD6, IGF1R, CBLB, HIF1A, CDKN2A, RAC2, ITGA6, VEGFA, GNB5, MTOR
Central carbon metabolism in cancer	7	0.0176	3.28E-04	PDK1, HIF1A, GLS, MET, PIK3CD, MTOR, SLC7A5
Proteoglycans in cancer	11	0.0276	7.08E-04	IGF1R, CAV1, CBLB, HIF1A, MAPK12, MET, VEGFA, PIK3CD, MTOR, MSN, FZD6
Focal adhesion	11	0.0276	0.0011	IGF1R, CAV1, RAC2, ITGA6, TNC, MET, VEGFA, PIK3CD, COL5A3, COL11A1, COL5A1
MicroRNAs in cancer	9	0.0226	0.0012	CDKN2A, GLS, TNC, MET, VEGFA, TP63, MTOR, HMGA2, DNMT3B
PI3K-Akt signaling pathway	14	0.0352	0.0017	TNC, MET, PIK3CD, FGF11, LPAR3, LPAR2, COL5A3, COL5A1, IGF1R, ITGA6, VEGFA, GNB5, MTOR, COL11A1
Ras signaling pathway	10	0.0251	0.0057	IGF1R, RAC2, ETS1, HTR7, MET, VEGFA, PIK3CD, FGF11, GNB5, ABL2

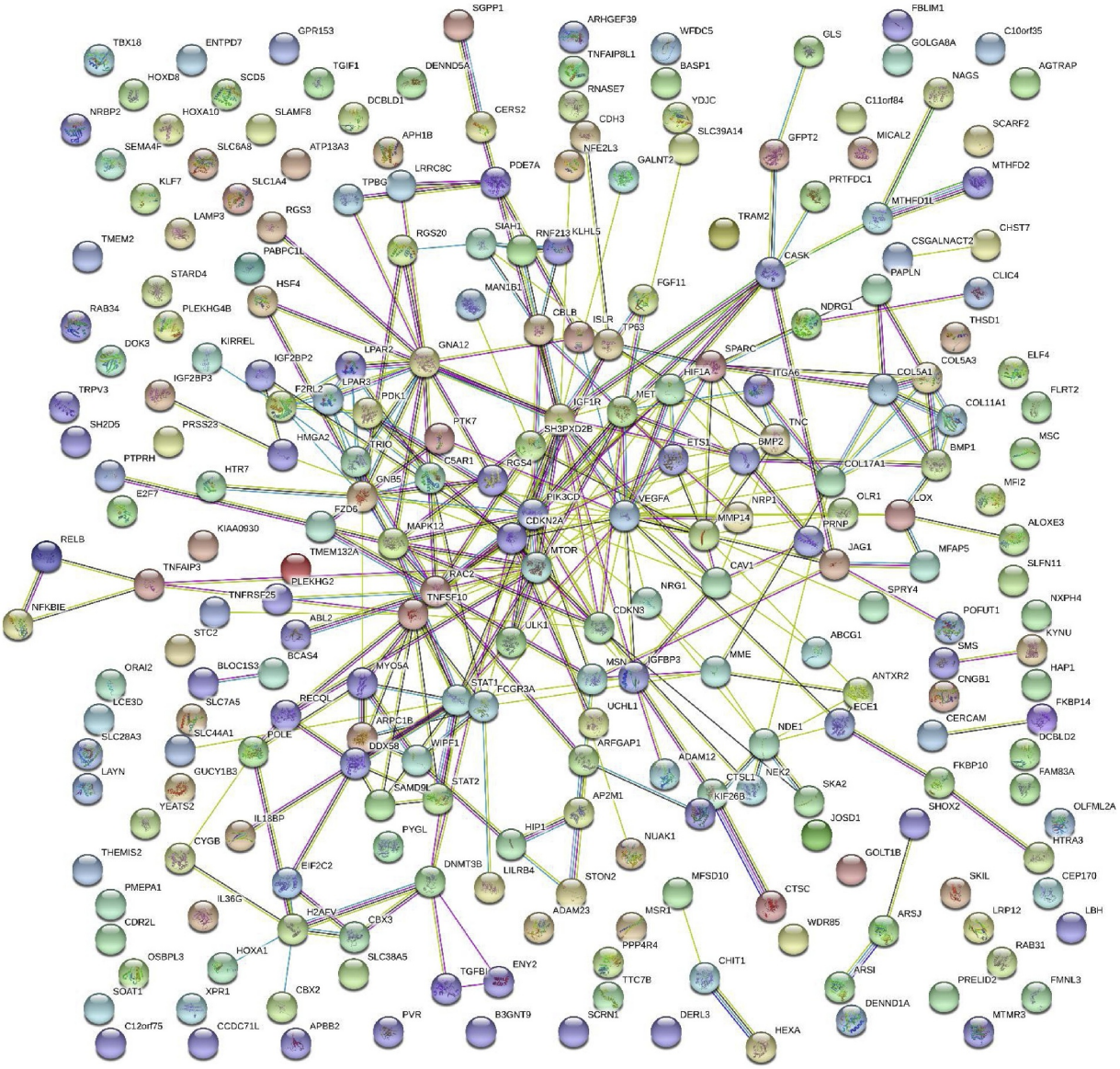

Fig. 9. PPI network of miR-99a-3p target genes in HNSCC.

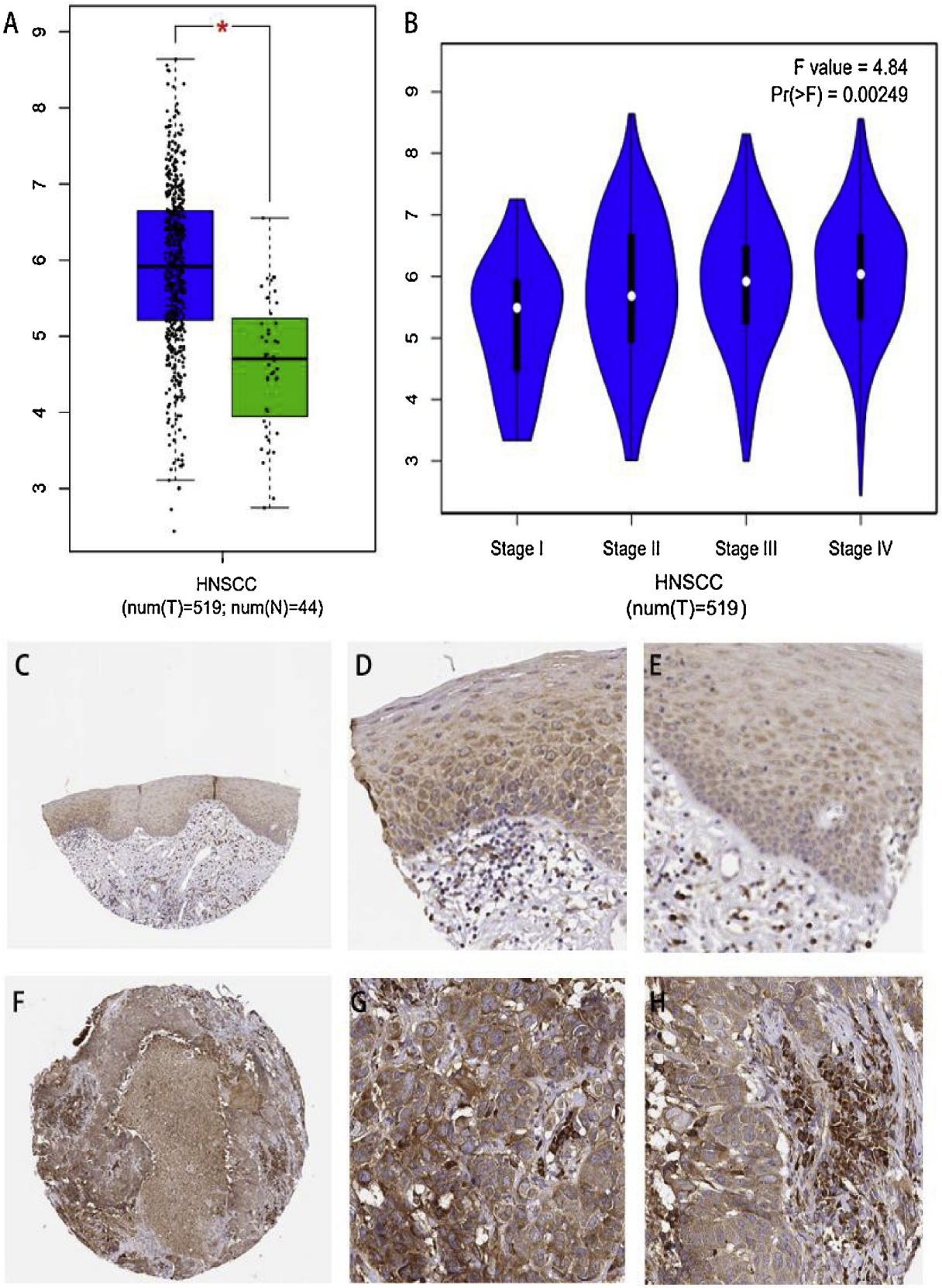

Fig. 10. Clinical value of a potential target gene, vascular endothelial growth factor A (VEGFA), of miR-99a-3p in HNSCC (A is mRNA level of VEGFA from TCGA and GTEx datasets; B is mRNA level of VEGFA in different clinical stages of HNSCC; Protein level of VEGFA stained by immunohistochemistry with the antibody CAB039240 in. C (x40), D, E (x400): normal squamous epithelial cells from upper aerodigestive tract mucosa, weak staining; F (x40), G, H (x400), HNSCC cells, moderate staining.

Disclosure of conflict of interest

None.

Acknowledgement

The authors sincerely appreciated the public databases: GEO, ArrayExpress and TCGA. The authors also thanked Dr. Xiao-jv Wu for the manuscript editing.

References

[1] S. Lopez-Verdin, J. Lavalle-Carrasco, R.G. Carreon-Burciaga, N. Serafin-Higuera, N. Molina-Frechero, R. Gonzalez-Gonzalez, R. Bologna-Molina, Molecular markers of anticancer drug resistance in head and neck squamous cell carcinoma: a literature review, Cancers 10 (2018).
[2] L. Zhao, W. Chi, H. Cao, W. Cui, W. Meng, W. Guo, B. Wang, Screening and clinical significance of tumor markers in head and neck squamous cell carcinoma through bioinformatics analysis, Mol. Med. Rep. (2018).
[3] C.Z. Xu, C. Jiang, Q. Wu, L. Liu, X. Yan, R. Shi, A feed-forward regulatory loop between HuR and the long noncoding RNA HOTAIR promotes head and neck squamous cell carcinoma progression and metastasis, Cell. Physiol. Biochem. 40 (2016) 1039–1051.
[4] R. Shimizu, S. Ibaragi, T. Eguchi, D. Kuwajima, S. Kodama, T. Nishioka, T. Okui, K. Obata, K. Takabatake, H. Kawai, K. Ono, K. Okamoto, H. Nagatsuka, A. Sasaki, Nicotine promotes lymph node metastasis and cetuximab resistance in head and neck squamous cell carcinoma, Int. J. Oncol. (2018).
[5] X. Pang, Y.L. Tang, X.H. Liang, Transforming growth factor-beta signaling in head and neck squamous cell carcinoma: insights into cellular responses, Oncol. Lett. 16 (2018) 4799–4806.
[6] P. Kozakiewicz, L. Grzybowska-Szatkowska, Application of molecular targeted therapies in the treatment of head and neck squamous cell carcinoma, Oncol. Lett. 15 (2018) 7497–7505.
[7] S. Emmett, D.C. Whiteman, B.J. Panizza, A. Antonsson, An update on cellular MicroRNA expression in human papillomavirus-associated head and neck squamous cell carcinoma, Oncology 95 (2018) 193–201.
[8] S. Shen, J. Bai, Y. Wei, G. Wang, Q. Li, R. Zhang, W. Duan, S. Yang, M. Du, Y. Zhao, D.C. Christiani, F. Chen, A seven-gene prognostic signature for rapid determination of head and neck squamous cell carcinoma survival, Oncol. Rep. 38 (2017) 3403–3411.
[9] G. Zhao, Y. Fu, Z. Su, R. Wu, How long non-coding RNAs and MicroRNAs mediate the endogenous RNA network of head and neck squamous cell carcinoma: a comprehensive analysis, Cell. Physiol. Biochem. 50 (2018) 332–341.
[10] L. Chen, H. Sun, C. Wang, Y. Yang, M. Zhang, G. Wong, miRNA arm switching identifies novel tumour biomarkers, EBioMedicine (2018).
[11] Y.Y. Li, Y.W. Tao, S. Gao, P. Li, J.M. Zheng, S.E. Zhang, J. Liang, Y. Zhang, Cancer-associated fibroblasts contribute to oral cancer cells proliferation and metastasis via exosome-mediated paracrine miR-34a-5p, EBioMedicine 36 (2018) 209–220.
[12] L. Hui, H. Wu, N. Yang, X. Guo, X. Jang, Identification of prognostic microRNA candidates for head and neck squamous cell carcinoma, Oncol. Rep. 35 (2016) 3321–3330.
[13] Y. Yamada, K. Koshizuka, T. Hanazawa, N. Kikkawa, A. Okato, T. Idichi, T. Arai, S. Sugawara, K. Katada, Y. Okamoto, N. Seki, Passenger strand of miR-145-3p acts as a tumor-suppressor by targeting MYO1B in head and neck squamous cell carcinoma, Int. J. Oncol. 52 (2018) 166–178.
[14] H. Wu, P. Pang, M.D. Liu, S. Wang, S. Jin, F.Y. Liu, C.F. Sun, Upregulated miR20a5p expression promotes proliferation and invasion of head and neck squamous cell carcinoma cells by targeting of TNFRSF21, Oncol. Rep. 40 (2018) 1138–1146.
[15] S. Molina-Pinelo, A. Carnero, F. Rivera, P. Estevez-Garcia, J.M. Bozada, M.L. Limon, M. Benavent, J. Gomez, M.D. Pastor, M. Chaves, R. Suarez, L. Paz-Ares, F. de la Portilla, A. Carranza-Carranza, I. Sevilla, L. Vicioso, R. Garcia-Carbonero, MiR-107 and miR-99a-3p predict chemotherapy response in patients with advanced colorectal cancer, BMC Cancer 14 (2014) 656.
[16] H. Xiong, Q. Li, S. Liu, F. Wang, Z. Xiong, J. Chen, H. Chen, Y. Yang, X. Tan, Q. Luo, J. Peng, G. Xiao, Q. Jiang, Integrated microRNA and mRNA transcriptome sequencing reveals the potential roles of miRNAs in stage I endometrioid endometrial carcinoma, PLoS One 9 (2014) e110163.
[17] H.B. Yan, Y. Zhang, J.M. Cen, X. Wang, B.L. Gan, J.C. Huang, J.Y. Li, Q.H. Song, S.H. Li, G. Chen, Expression of microRNA-99a-3p in prostate Cancer Based on bioinformatics data and meta-analysis of a literature review of 965 cases, Med. Sci. Monit. 24 (2018) 4807–4822.
[18] T. Arai, A. Okato, Y. Yamada, S. Sugawara, A. Kurozumi, S. Kojima, K. Yamazaki, Y. Naya, T. Ichikawa, N. Seki, Regulation of NCAPG by miR-99a-3p (passenger strand) inhibits cancer cell aggressiveness and is involved in CRPC, Cancer Med. 7 (2018) 1988–2002.
[19] M. Haeussler, A.S. Zweig, C. Tyner, M.L. Speir, K.R. Rosenbloom, B.J. Raney, C.M. Lee, B.T. Lee, A.S. Hinrichs, J.N. Gonzalez, D. Gibson, M. Diekhans, H. Clawson, J. Casper, G.P. Barber, D. Haussler, R.M. Kuhn, W.J. Kent, The UCSC genome browser database: 2019 update, Nucleic Acids Res. (2018).
[20] C. Tyner, G.P. Barber, J. Casper, H. Clawson, M. Diekhans, C. Eisenhart, C.M. Fischer, D. Gibson, J.N. Gonzalez, L. Guruvadoo, M. Haeussler, S. Heitner, A.S. Hinrichs, D. Karolchik, B.T. Lee, C.M. Lee, P. Nejad, B.J. Raney, K.R. Rosenbloom, M.L. Speir, C. Villarreal, J. Vivian, A.S. Zweig, D. Haussler, R.M. Kuhn, W.J. Kent, The UCSC genome browser database: 2017 update, Nucleic Acids Res. 45 (2017) D626–D634.
[21] M.S. Cline, B. Craft, T. Swatloski, M. Goldman, S. Ma, D. Haussler, J. Zhu, Exploring TCGA pan-cancer data at the UCSC Cancer, Genomics Browser, Sci Rep 3 (2013) 2652.
[22] Y.Y. Liang, J.C. Huang, R.X. Tang, W.J. Chen, P. Chen, W.L. Cen, K. Shi, L. Gao, X. Gao, A.G. Liu, X.T. Peng, G. Chen, S.N. Huang, Y.Y. Fang, Y.Y. Gu, Clinical value of miR-198-5p in lung squamous cell carcinoma assessed using microarray and RT-qPCR, World J. Surg. Oncol. 16 (2018) 22.
[23] C. Sticht, C. De La Torre, A. Parveen, N. Gretz, miRWalk: an online resource for prediction of microRNA binding sites, PLoS One 13 (2018) e0206239.
[24] Z. Tang, C. Li, B. Kang, G. Gao, C. Li, Z. Zhang, GEPIA: a web server for cancer and normal gene expression profiling and interactive analyses, Nucleic Acids Res. 45 (2017) W98–W102.
[25] C. Huang, N. Yuan, L. Wu, X. Wang, J. Dai, P. Song, F. Li, C. Xu, X. Zhao, An integrated analysis for long noncoding RNAs and microRNAs with the mediated competing endogenous RNA network in papillary renal cell carcinoma, Onco. Ther. 10 (2017) 4037–4050.
[26] L. Gao, S.H. Li, Y.X. Tian, Q.Q. Zhu, G. Chen, Y.Y. Pang, X.H. Hu, Role of down-regulated miR-133a-3p expression in bladder cancer: a bioinformatics study, Onco. Ther. 10 (2017) 3667–3683.
[27] M. Pathan, S. Keerthikumar, C.S. Ang, L. Gangoda, C.Y. Quek, N.A. Williamson, D. Mouradov, O.M. Sieber, R.J. Simpson, A. Salim, A. Bacic, A.F. Hill, D.A. Stroud, M.T. Ryan, J.I. Agbinya, J.M. Mariadason, A.W. Burgess, S. Mathivanan, FunRich: an open access standalone functional enrichment and interaction network analysis tool, Proteomics 15 (2015) 2597–2601.
[28] X. You, S. Yang, J. Sui, W. Wu, T. Liu, S. Xu, Y. Cheng, X. Kong, G. Liang, Y. Yao, Molecular characterization of papillary thyroid carcinoma: a potential three-lncRNA prognostic signature, Cancer Manag. Res. 10 (2018) 4297–4310.
[29] Z. Zhang, C. Fang, Y. Wang, J. Zhang, J. Yu, Y. Zhang, X. Wang, J. Zhong, COL1A1: a potential therapeutic target for colorectal cancer expressing wild-type or mutant KRAS, Int. J. Oncol. 53 (2018) 1869–1880.
[30] D.Y. Wen, D.H. Pan, P. Lin, Q.Y. Mo, Y.P. Wei, Y.H. Luo, G. Chen, Y. He, J.Q. Chen, H. Yang, Downregulation of miR4865p in papillary thyroid carcinoma tissue: a study based on microarray and miRNA sequencing, Mol. Med. Rep. 18 (2018) 2631–2642.
[31] X. Ma, R. Tao, L. Li, H. Chen, Z. Liu, J. Bai, X. Shuai, C. Wu, K. Tao, Identification of a 5microRNA signature and hub miRNAmRNA interactions associated with pancreatic cancer, Oncol. Rep. (2018).
[32] X. Zhang, H. Feng, Z. Li, D. Li, S. Liu, H. Huang, M. Li, Application of weighted gene co-expression network analysis to identify key modules and hub genes in oral squamous cell carcinoma tumorigenesis, Onco. Ther. 11 (2018) 6001–6021.
[33] H.T. Xu, J.C. Guo, H.Z. Liu, W.W. Jin, A time-series analysis of severe burned injury of skin gene expression profiles, Cell. Physiol. Biochem. 49 (2018) 1492–1498.
[34] B. Han, D. Feng, X. Yu, Y. Zhang, Y. Liu, L. Zhou, Identification and interaction analysis of molecular markers in colorectal Cancer by integrated bioinformatics analysis, Med. Sci. Monit. 24 (2018) 6059–6069.
[35] C. Meng, X. Shen, W. Jiang, Potential biomarkers of HCC based on gene expression and DNA methylation profiles, Oncol. Lett. 16 (2018) 3183–3192.
[36] X. Wang, H. Zhao, X. Wu, G. Xi, S. Zhou, Tangshen formula treatment for diabetic kidney disease by inhibiting Racgap1-stata5-Mediated cell proliferation and restoring miR-669j-Arntl-Related circadian rhythm, Med. Sci. Monit. 24 (2018) 7914–7928.
[37] W. Cui, Z. Gu, H. Liu, C. Zhang, J. Liu, Identification modules of gastric cancer based on protein-protein interaction networks and gene expression data, J. BUON 23 (2018) 1013–1019.
[38] Y. Pan, Y. Zhang, J. Liu, Text miningbased drug discovery in cutaneous squamous cell carcinoma, Oncol. Rep. (2018).
[39] X. Tang, Y. Xu, L. Lu, Y. Jiao, J. Liu, L. Wang, H. Zhao, Identification of key candidate genes and small molecule drugs in cervical cancer by bioinformatics strategy, Cancer Manag. Res. 10 (2018) 3533–3549.
[40] M. Uhlen, L. Fagerberg, B.M. Hallstrom, C. Lindskog, P. Oksvold, A. Mardinoglu, A. Sivertsson, C. Kampf, E. Sjostedt, A. Asplund, I. Olsson, K. Edlund, E. Lundberg, S. Navani, C.A. Szigyarto, J. Odeberg, D. Djureinovic, J.O. Takanen, S. Hober, T. Alm, P.H. Edqvist, H. Berling, H. Tegel, J. Mulder, J. Rockberg, P. Nilsson, J.M. Schwenk, M. Hamsten, K. von Feilitzen, M. Forsberg, L. Persson, F. Johansson, M. Zwahlen, G. von Heijne, J. Nielsen, F. Ponten, Proteomics. Tissue-based map of the human proteome, Science 347 (2015) 1260419.
[41] P.J. Thul, L. Akesson, M. Wiking, D. Mahdessian, A. Geladaki, H. Ait Blal, T. Alm, A. Asplund, L. Bjork, L.M. Breckels, A. Backstrom, F. Danielsson, L. Fagerberg, J. Fall, L. Gatto, C. Gnann, S. Hober, M. Hjelmare, F. Johansson, S. Lee, C. Lindskog, J. Mulder, C.M. Mulvey, P. Nilsson, P. Oksvold, J. Rockberg, R. Schutten, J.M. Schwenk, A. Sivertsson, E. Sjostedt, M. Skogs, C. Stadler, D.P. Sullivan, H. Tegel, C. Winsnes, C. Zhang, M. Zwahlen, A. Mardinoglu, F. Ponten, K. von Feilitzen, K.S. Lilley, M. Uhlen, E. Lundberg, A subcellular map of the human proteome, Science 356 (2017).
[42] M. Uhlen, C. Zhang, S. Lee, E. Sjostedt, L. Fagerberg, G. Bidkhori, R. Benfeitas, M. Arif, Z. Liu, F. Edfors, K. Sanli, K. von Feilitzen, P. Oksvold, E. Lundberg, S. Hober, P. Nilsson, J. Mattsson, J.M. Schwenk, H. Brunnstrom, B. Glimelius, T. Sjoblom, P.H. Edqvist, D. Djureinovic, P. Micke, C. Lindskog, A. Mardinoglu, F. Ponten, A pathology atlas of the human cancer transcriptome, Science (2017) 357.
[43] G. Gremel, D. Djureinovic, M. Niinivirta, A. Laird, O. Ljungqvist, H. Johannesson, J. Bergman, P.H. Edqvist, S. Navani, N. Khan, T. Patil, A. Sivertsson, M. Uhlen, D.J. Harrison, G.J. Ullenhag, G.D. Stewart, F. Ponten, A systematic search strategy

identifies cubilin as independent prognostic marker for renal cell carcinoma, BMC Cancer 17 (9) (2017).
[44] K. Magnusson, G. Gremel, L. Ryden, V. Ponten, M. Uhlen, A. Dimberg, K. Jirstrom, F. Ponten, ANLN is a prognostic biomarker independent of Ki-67 and essential for cell cycle progression in primary breast cancer, BMC Cancer 16 (2016) 904.
[45] A. Schluter, P. Weller, O. Kanaan, I. Nel, L. Heusgen, B. Hoing, P. Hasskamp, S. Zander, M. Mandapathil, N. Dominas, J. Arnolds, B.A. Stuck, S. Lang, A. Bankfalvi, S. Brandau, CD31 and VEGF are prognostic biomarkers in early-stage, but not in late-stage, laryngeal squamous cell carcinoma, BMC Cancer 18 (2018) 272.
[46] C.B. Sales, M.E. Buim, R.O. de Souza, L. de Faro Valverde, M.C. Mathias Machado, M.G. Reis, F.A. Soares, E.A. Ramos, C.A. Gurgel Rocha, Elevated VEGFA mRNA levels in oral squamous cell carcinomas and tumor margins: a preliminary study, J. Oral Pathol. Med. 45 (2016) 481–485.
[47] M.P. Sablin, C. Dubot, J. Klijanienko, S. Vacher, L. Ouafi, W. Chemlali, M. Caly, X. Sastre-Garau, E. Lappartient, O. Mariani, J. Rodriguez, T. Jouffroy, A. Girod, V. Calugaru, C. Hoffmann, R. Lidereau, F. Berger, M. Kamal, I. Bieche, C. Le Tourneau, Identification of new candidate therapeutic target genes in head and neck squamous cell carcinomas, Oncotarget 7 (2016) 47418–47430.